Brain **118**, 401 (1995); J. V. Haxby *et al.*, *Proc. Natl. Acad. Sci. U.S.A.* **93**, 922 (1996).

29. Experiments were conducted in accordance with the NIH *Guide for the Care and Use of Laboratory Animals* and with the regulations of the University of Tokyo School of Medicine. This work was supported by grants from Research Fellowships of the Japan Society for the Promotion of Science for Young Scientists to I.H. and T.I. and by a grant-in-aid for Specially Promoted Research from the Ministry for Education, Science, and Culture of Japan (07102006) to Y.M. We thank S. Konishi and M. Kameyama for collaboration; H. Niki for helpful discussion; C. Hamada for statistical assistance; T. Kitamura, J. Yamada, M. Yukie, and M. Yoshida for histological advice; and T. Kirino for encouragement.

24 March 1998; accepted 10 June 1998

Coupled Gating Between Individual Skeletal Muscle Ca^{2+} Release Channels (Ryanodine Receptors)

Steven O. Marx, Karol Ondrias, Andrew R. Marks*

Excitation-contraction coupling in skeletal muscle requires the release of intracellular calcium ions (Ca^{2+}) through ryanodine receptor (RyR1) channels in the sarcoplasmic reticulum. Half of the RyR1 channels are activated by voltage-dependent Ca^{2+} channels in the plasma membrane. In planar lipid bilayers, RyR1 channels exhibited simultaneous openings and closings, termed "coupled gating." Addition of the channel accessory protein FKBP12 induced coupled gating, and removal of FKBP12 uncoupled channels. Coupled gating provides a mechanism by which RyR1 channels that are not associated with voltage-dependent Ca^{2+} channels can be regulated.

Intracellular Ca^{2+} release channels, present in the endoplasmic (or sarcoplasmic) reticulum of virtually all cells, are integral to diverse signaling pathways that require translation of electrical or biochemical extracellular signals into intracellular activation of Ca^{2+}-dependent molecules. The Ca^{2+} release channels in skeletal muscle comprise four 565-kD type 1 RyR subunits and four molecules of the 12-kD protein FKBP12 (*1*). FKBP12, which stabilizes the RyR1 complex and enables the four subunits to open and close coordinately (*2*), is a member of the immunophilin family of cis-trans peptidyl-prolyl isomerases that serve as cytosolic receptors for immunosuppressant drugs including rapamycin and FK506 (*3*).

Recombinant RyR1 expressed in insect (Sf9) cells in the absence of FKBP12 forms channels with multiple subconductance states, consistent with a defect in coordination of the activity of the four channel subunits (*2*). Addition of FKBP12 to recombinant RyR1 stabilizes the channel complex, resulting in the formation of channels with full conductance (*2*). This stabilizing effect is reversed by treating the channels with rapamycin or FK506 to remove FKBP12 from RyR1 (*2*).

The cytosolic domain of RyR1 projects into the space that separates the transverse tubule (T-tubule) and the sarcoplasmic reticulum (SR). A cytosolic domain of the $\alpha 1$ subunit of voltage-dependent Ca^{2+} channels (VDCCs) in the T-tubule is required for activation of RyR1 during excitation-contraction (E-C) coupling (*4*). Fragments of this domain can activate or inactivate RyR1 (*5–7*), indicating that E-C coupling may involve a protein-protein interaction between the two types of Ca^{2+} channels. Clusters of four VDCCs in the T-tubule overlie only every other RyR1 channel (*8*). Thus, a cytosolic loop from a VDCC is directly apposed to each subunit of only half of the RyR1 channels.

Recombinant RyR1 coexpressed with FKBP12 in Sf9 cells formed Ca^{2+}-activated Ca^{2+} channels that exhibited stable openings to 4 pA in planar lipid bilayers (Fig. 1A) (*2*). A current amplitude histogram (Fig. 1D) revealed two discrete peaks corresponding to closed channels (0 pA) and openings to the full amplitude of a single channel (4 pA). In some experiments (9 of 44), two channels opening and closing (gating) independently in the same bilayer were observed (Fig. 1B). In these experiments, one channel opened to the 4-pA level and a second channel was clearly apparent, opening independently of the first. A current amplitude histogram (Fig. 1E) revealed three discrete peaks corresponding to closed channels (0 pA) and openings to the full amplitude for one channel (4 pA) or for two channels (8 pA).

The single-channel properties of recombinant RyR1 coexpressed with FKBP12 were identical to those of native RyR1 from SR vesicles (*2*). The native RyR1 exhibited the typical current amplitude of 4 pA (Fig. 2, A and B). In some experiments (12 of 56), two channels were observed in the bilayer (Fig. 2B); channel openings to the 4-pA level and a second channel opening to 8 pA were apparent. A current amplitude histogram (Fig. 2E) revealed three discrete peaks corresponding to closed channels (0 pA) and openings to 4 and 8 pA.

In ~10% of experiments with either recombinant (4 of 44) (Fig. 1C) or native (5 of 56) (Fig. 2C) RyR1, channels were observed that opened to 8 pA, twice the normal current amplitude. Current amplitude histograms (Figs. 1F and 2F) revealed two discrete peaks corresponding to closed channels (0 pA) and openings to 8 pA. RyR1 channels exhibit a conductance of ~100 pS when Ca^{2+} (50 mM) is the current carrier at 0 mV (*9*). The conductances were 93 ± 18 pS for the single-amplitude openings and 180 ± 20 pS for the double-amplitude openings (Fig. 1G).

If both the 4-pA and the 8-pA openings represented activity of two independent RyR1 channels in the bilayer, then the binomial distribution of open probabilities would provide a calculated open probability ($P1_{calc}$) for the 4-pA current equal to the experimental value *P1*. The probability of the 4-pA openings in Fig. 1B predicted by a binomial distribution ($P1_{calc}$) equalled the experimentally observed value *P1* ($P > 0.05$, Student's *t* test). The same analysis applied to the open probabilities of currents in Fig. 1C showed that $P1_{calc}$ did not match the experimentally observed value for *P1* ($P < 0.001$, Student's *t* test). The failure of a binomial distribution based on the open probability of the 8-pA currents (*P2*) in Fig. 1C to predict the open probability of the 4-pA currents (*P1*) indicates that the 8-pA currents did not result from openings of two independent channels (*10*). Thus, the gating of two channels in Fig. 1C was likely coupled. Application of the binomial distribution is limited by the fact that it cannot distinguish between the presence of two interdependent cooperative channels each exhibiting a 4-pA current only, and that of a single channel with current amplitudes of 4 and 8 pA. However, if the actual current amplitude for RyR1 is 8 pA, the conductance of the channel would be exactly twice that measured for RyR1 in previous studies (*2, 11, 12*). Moreover, the 8-pA cur-

S. O. Marx, Molecular Cardiology Program, Divisions of Cardiology and Circulatory Physiology, Department of Medicine, Columbia University College of Physicians and Surgeons, New York, NY 10032, USA. K. Ondrias, Institute of Molecular Physiology and Genetics, Slovak Academy of Sciences, Bratislava 83334, Slovak Republic. A. R. Marks, Molecular Cardiology Program, Divisions of Cardiology and Circulatory Physiology, Department of Medicine, and Department of Pharmacology, Columbia University College of Physicians and Surgeons, New York, NY 10032, USA.

*To whom correspondence should be addressed. E-mail: arm42@columbia.edu

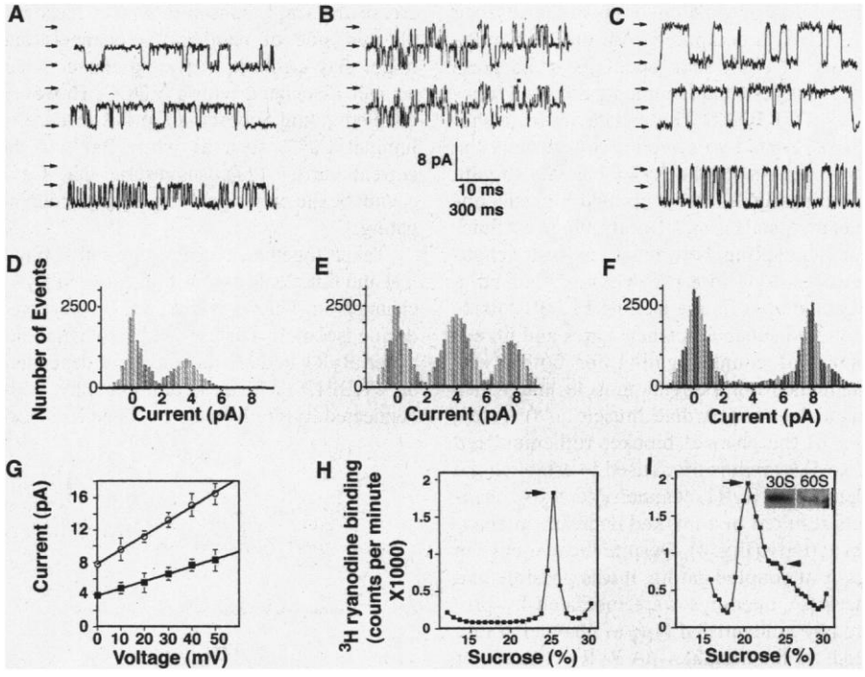

Fig. 1. Coupled gating of channels formed from recombinant skeletal muscle RyR1 coexpressed with FKBP12. (**A**) A single recombinant RyR1 channel with openings to 4 pA. Liposomes (*22*) were fused to planar lipid bilayers (*23*), and channels were activated with 1 mM caffeine. (**B**) Recording from two independent channels. (**C**) RyR1 channels opening to 8 pA. The time scales are expanded in the top two traces in (A) through (C) and compressed in the bottom trace in (A) and (C). Recordings were made at 0 mV, channel openings are in the upward direction, and the arrows at the left of the traces in (A) through (C) indicate (from bottom to top, respectively) the 0-, 4-, and 8-pA current levels. (**D** through **F**) Current amplitude histograms of channels shown in (A) through (C), respectively. (**G**) Current-voltage relations for the channel in (A) (■) and the coupled channels in (C) (○). Data are means ± SD. (**H** and **I**) Physical association between RyR1 Ca^{2+} release channels was demonstrated by centrifugation of high density SR from skeletal muscle, after incubation with [^{3}H]ryanodine and solubilization with CHAPS detergent, through 10 to 32% (w/v) linear sucrose density gradients (*2*) for 17 or 10 hours, respectively. In (H), the 25% sucrose fraction contained the 30*S* RyR1 complex (arrow), and ~60*S* complexes were in the pellet. In (I), the 30*S* complex (arrow) was present in the 20% sucrose fraction, and an ~60*S* complex (arrowhead) was present in the 24% sucrose fraction. The inset in (I) shows immunoblot analysis of samples from the 20% (30*S*) and 24% (60*S*) sucrose fractions with specific antibodies to RyR1 (*9*). Coomassie staining showed that these fractions contained a single high molecular weight protein (*17*). Only the bottom portion of each gradient is shown, fraction 1 being the top of the gradient. Data are representative of six similar experiments.

rents showed the same biophysical properties (including dwell times and open probabilities) and responded to pharmacological modulators of RyR1 in exactly the same manner as did the 4-pA currents (*13*).

Ultrastructural studies of skeletal muscle have shown that RyR1 channels are tightly clustered square structures arrayed in regular rows, and that the corners of adjacent channels contact one another (*14, 15*). Coupled gating was observed in ~10% of experiments with either recombinant or native RyR1 channels. Electron micrographs of purified RyR1 homotetramers show that ~10% of these structures are physically connected to form contacting pairs (*14*). We incubated high density SR with [^{3}H]ryanodine and, after solubilization, subjected the preparation to sucrose density gradient centrifugation under conditions designed to separate individual 30*S* RyR1 homotetramers from dimers of two physically associated channels that sediment at ~60*S* (*16*). Approximately 10% of the RyR1 channels from high density SR preparations sedimented at ~60*S*, corresponding to two physically associated RyR1 channels (Fig. 1, H and I). Specific [^{3}H]ryanodine binding was also detected in fractions with sedimentation coefficients of >60*S*, suggesting that more than two RyR1 homotetramers can remain physically connected during purification. We have observed 12-, 16-, and 20-pA openings, indicative of coupled gating of three, four, and five channels, respectively (*17*). The physical association of RyR1 channels was not affected by removal of FKBP12 (*17*).

In experiments in which RyR1 was expressed in insect cells in the absence of FKBP12 (Sf9 cells do not contain FKBP12), subconductance states (openings to <4 pA) (*2*) were observed. In some of these experiments (3 of 44), both subconductance states and rare openings with currents of >4 pA were observed (Fig. 3A). A current amplitude histogram (Fig. 3E) revealed a distribution of events with currents from 1 to 8 pA, consistent with the presence of two uncoupled channels. Addition of FKBP12 eliminated subconductance states and induced stable openings to 8 pA (Fig. 3B). A current amplitude histogram (Fig. 3F) revealed two discrete peaks corresponding to closed channels (0 pA) and openings to 8 pA, consistent with coupled gating of two channels.

Amplitude histograms (Fig. 3, E and F) showed that the probability of 8-pA openings increased markedly in the presence of FKBP12. Effective removal of FKBP12 by the addition of rapamycin (2 μM) induced two coupled RyR1 channels (Fig. 3, C and G) to uncouple (Fig. 3, D and H). The low

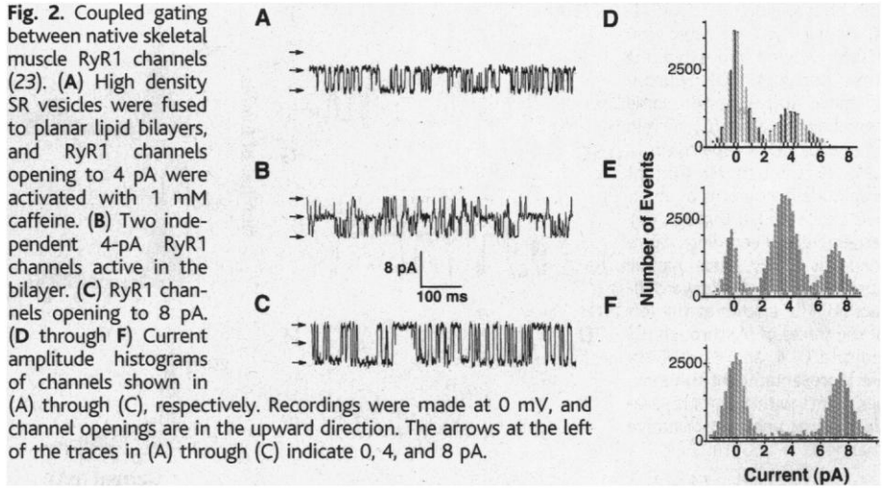

Fig. 2. Coupled gating between native skeletal muscle RyR1 channels (*23*). (**A**) High density SR vesicles were fused to planar lipid bilayers, and RyR1 channels opening to 4 pA were activated with 1 mM caffeine. (**B**) Two independent 4-pA RyR1 channels active in the bilayer. (**C**) RyR1 channels opening to 8 pA. (**D** through **F**) Current amplitude histograms of channels shown in (A) through (C), respectively. Recordings were made at 0 mV, and channel openings are in the upward direction. The arrows at the left of the traces in (A) through (C) indicate 0, 4, and 8 pA.

probability of 8-pA openings in the absence of FKBP12, compared with the high probability of eight such openings in its presence, suggests that coupled gating is a function of FKBP12. These data indicate that FKBP12 has two effects: (i) it permits the four subunits of the RyR1 channel to gate coordinately, thereby eliminating subconductance states, and (ii) it enhances functional coupling between two RyR1 channels, resulting in 8-pA openings. Indeed, a recent study of mice lacking FKBP12 demonstrated subconductance states and no evidence of coupled gating for both RyR1 channels from skeletal muscle and RyR2 channels from cardiac muscle (*18*). Addition of the channel blocker ruthenium red (5 μM), which is often used to establish the identity of RyR1 channels, to 8-pA channels resulted in a marked decrease in channel activity (Fig. 4). Despite the evidence in favor of coupled gating, it was possible that the 8-pA openings were mediated by previously unidentified type of channel, a rare mode of the normal 4-pA RyR1 channel, or a partially degraded form of the normal channel. These possibilities were rendered less likely by the fact that coupled gating was not observed in 10 experiments with 30*S* RyR1 channels isolated by sucrose density gradient centrifugation, but it was observed in four experiments with purified RyR1 channels reconstituted from the 60*S* complex (*17*).

Coupled gating, modulated by FKBP12, is compatible with previous observations supporting a role for Ca^{2+}-induced Ca^{2+} release in skeletal muscle (*19–21*). The movement of Ca^{2+} through one RyR1 channel should increase the Ca^{2+} concentration on the cytoplasmic side of neighboring channels and might play a role in activating channels that are not associated with a VDCC. However, coupled gating is observed in the absence of luminal Ca^{2+}, such as when Ba^{2+} is the current carrier (*17*), suggesting that Ca^{2+} cannot be the only signal required for coupled gating.

Taken together, our data show that physical and functional association between RyR1 channels in skeletal muscle can be preserved during isolation. The physical association between RyR1 homotetramers is not dependent on FKBP12 (*17*). Two or more physically connected RyR1 channels can open and close simultaneously. The functional association between RyR1 channels, which we have termed coupled gating, is enhanced by FKBP12. In skeletal muscle, the T-tubule–SR junctions are discontinuous such that each junction forms a discrete subset of all of the RyR1 channels in a skeletal myotube. Through coupled gating, activation of one RyR1 channel might activate all of the RyR1 channels in a junction. In skeletal muscle, the T-tubule–SR junctions are discontinuous such that each junction forms a discrete subset of all the RyR1 channels in a skeletal myotube. Through coupled gating, activation of one RyR1 channel might activate all of the RyR1 channels in a junction. Coupled gating provides a mechanism for the concerted activation of RyR1 Ca^{2+} release channels during skeletal muscle E-C coupling.

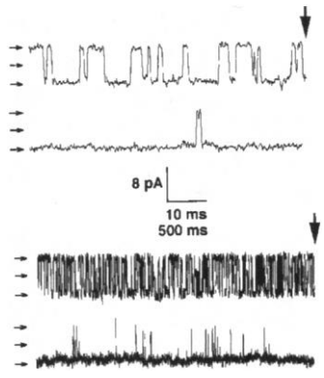

Fig. 4. Inhibition of coupled native skeletal muscle RyR1 channel activity by ruthenium red (5 μM). Vertical arrows indicate the addition of ruthenium red. Recordings were made at 0 mV, and channel openings are in the upward direction. Arrows at the left indicate 0, 4, and 8 pA. Time calibration is 10 ms in upper traces and 500 ms in lower traces.

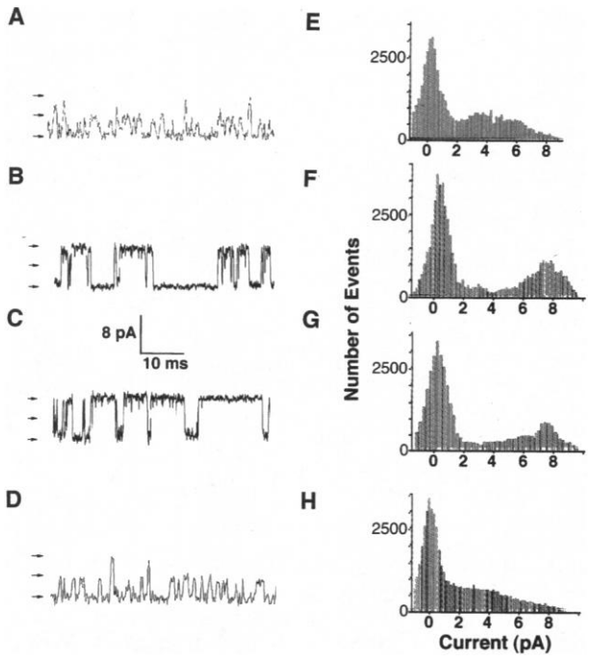

Fig. 3. Requirement of FKBP12 for coupled gating of RyR1 channels. (**A**) Two recombinant RyR1 channels (expressed without FKBP12) activated with 1 mM caffeine. (**B**) The same two channels as in (A) 30 min after addition of FKBP12. (**C**) Native RyR1 activated with 1 mM caffeine and exhibiting 8-pA openings. (**D**) Subconductance states of the same two channels as in (C) 10 min after addition of rapamycin (2 μM). (**E** through **H**) Current amplitude histograms of channels shown in (A) through (D), respectively. Recordings were made at 0 mV, and channel openings are in the upward direction. The arrows at the left of the traces in (A) through (D) indicate 0, 4, and 8 pA. Data are representative of three experiments with three preparations of recombinant or native channels.

References and Notes

1. T. Jayaraman *et al.*, *J. Biol. Chem.* **267**, 9474 (1992).
2. A.-M. B. Brillantes *et al.*, *Cell* **77**, 513 (1994).
3. S. L. Schreiber, *Science* **251**, 283 (1991).
4. T. Tanabe, K. G. Beam, B. A. Adams, T. Niidome, S. Numa, *Nature* **346**, 567 (1990).
5. X. Lu, L. Xu, G. Meissner, *J. Biol. Chem.* **269**, 6511 (1994).
6. ———, *ibid.* **270**, 18459 (1995).
7. R. el-Hayek, B. Antoniu, J. Wang, S. L. Hamilton, N. Ikemoto, *ibid.*, p. 22116.
8. C. Franzini-Armstrong and J. W. Kish, *J. Muscle Res. Cell Motil.* **16**, 319 (1995).
9. K. Ondrias, A.-M. B. Brillantes, A. Scott, B. E. Ehrlich, A. R. Marks, *Organell. Ion Channels Transport.* **51**, 29 (1996).
10. D. O. Mak and J. K. Foskett, *J. Gen. Physiol.* **109**, 571 (1997).
11. I. Bezprozvanny and B. E. Ehrlich, *ibid.* **104**, 821 (1994).
12. R. Coronado, S. Kawano, C. Lee, C. Valdivia, H. Valdivia, *Methods Enzymol.* **207**, 699 (1992).
13. Dwell-time distributions (in milliseconds, means ± SEM, n = 5) for the closed and open states corresponding to the 8-pA currents (mean closed times, τ_{1c} = 11.8 ± 1.8 and τ_{2c} = 1.9 ± 0.9; mean open times, τ_{1o} = 9.8 ± 1.2 and τ_{2o} = 1.3 ± 0.4) were indistinguishable ($P > 0.05$) from those of the 4-pA currents (mean closed times, τ_{1c} = 12.1 ± 1.1 and τ_{2c} = 2.4 ± 0.7; mean open times, τ_{1o} = 10.1 ± 1.5 and τ_{2o} = 1.4 ± 0.5). The biophysical properties of two coupled channels (8-pA openings) were identical to those of the single channels (4-pA openings), with the exception of the current amplitude. At the conclusion of experiments, ryanodine (1 μM), which locks RyR1 channels in a characteristic 50% subconductance state, was added to establish that the channels comprised RyR1 subunits. RyR channels are the only known channels that are affected in this manner by ryanodine [E. Rousseau, J. S. Smith, G. Meissner, *Am. J. Physiol.* **253**, C364 (1987)]. When ryanodine was added to two coupled channels, the current amplitude was reduced from 8 to 4 pA (two half-conducting channels, n = 9) (*16*). Addition of rapamycin (2 μM) uncoupled channels; after 10 to 20 min, multiple subconductance states appeared (n = 9). Both the 4- and 8-pA RyR1 currents were blocked by 5 μM ruthenium red (n = 5) (*16*), an inhibitor of the channel. Adjusting the cytosolic (cis) Ca^{2+} concentration from 50 nM to 1 μM had no effect on coupled gating. Coupled RyR1 channels responded to changes in the cytosolic (cis) Ca^{2+} concentration in the same manner as did uncoupled channels; they exhibited the same bell-shaped response [I. Bezprozvanny, J. Watras, B. Ehrlich, *Nature* **351**, 751 (1991)], being activated at ~250 nM Ca^{2+} and inhibited at millimolar concentrations of Ca^{2+}.

14. A. Saito, M. Inui, M. Radermacher, J. Frank, S. Fleischer, *J. Cell Biol.* **107**, 211 (1988).
15. B. A. Block, T. Imagawa, K. P. Campbell, C. Franzini-Armstrong, *ibid.*, p. 2587.
16. High density SR from skeletal muscle was incubated with [^{3}H]ryanodine, solubilized with CHAPS detergent, and centrifuged for 10 hours on a 10 to 32% linear sucrose gradient at 26,000 rpm and 2°C in a Sorvall AH-629 rotor (17-ml tubes) (*2*, *9*).
17. S. O. Marx, K. Ondrias, A. R. Marks, unpublished data.
18. W. Shou *et al.*, *Nature* **391**, 489 (1998).
19. M. Endo, M. Tanaka, Y. Ogawa, *ibid.* **228**, 34 (1970).
20. L. E. Ford and R. J. Podolsky, *Science* **167**, 58 (1970).
21. E. Ríos and G. Pizarro, *News Physiol. Sci.* **3**, 223 (1988).
22. Recombinant rabbit skeletal muscle RyR1 was expressed in Sf9 cells, purified by sucrose density gradient centrifugation, and reconstituted into liposomes, which were then fused to planar lipid bilayers (*2*, *9*). For some experiments, recombinant FKBP12 was expressed with RyR1 in Sf9 cells; in other experiments, 150 nM FKBP12 protein was added to the cis chamber after fusion, as described (*2*). Thirty minutes after addition of FKBP12 (or immediately in the case of RyR1 co-expressed with FKBP12), RyR1 was activated with caffeine (1 mM) or by adjusting the free Ca^{2+} concentration in the cis chamber to 250 nM.
23. SR vesicles were isolated from rabbit skeletal muscle and incorporated into planar lipid bilayers as described [F. A. Lai, H. P. Erickson, E. Rousseau, Q. L. Liu, G. Meissner, *Nature* **331**, 315 (1988)], with the following modifications: (i) Vesicles were isolated in buffer containing 150 mM KCl from the 32 to 40% (w/v) sucrose interface. (ii) Vesicles were incorporated immediately into planar lipid bilayers, such that fusion occurred instantly or within a few minutes, under high hydrostatic pressure. And (iii) solutions in the cis and trans chambers were supplemented with 50 mM KCl. For recordings from RyR1 channels, black lipid membranes were formed across a hole (diameter, 0.05 to 0.3 mm) separating the cis and trans chambers, as described [C. Miller, *Ion Channel Reconstitution* (Plenum, New York, 1986), pp. 3–151]. The voltage across the bilayer membrane was clamped at 0 mV, and the current carrier was Ca^{2+}. The cis solution contained 250 mM Hepes (pH 7.35), 125 mM tris, 50 mM KCl, 1.0 mM EGTA, and 0.7 mM $CaCl_2$, to give a free Ca^{2+} concentration of 250 nM; the trans solution contained 53 mM $Ca(OH)_2$, 250 mM Hepes (pH 7.35), and 50 mM KCl. The trans chamber was connected to the head-stage input of an Axon 200 amplifier (Axon Instruments, Foster City, CA) by a Ag-AgCl electrode and agar-KCl bridges. Single-channel currents were continuously monitored and recorded on a Digital Audio Tape (DAT) and with a chart recorder. Recordings were filtered through a low-pass Bessel device (Frequency Devices, Haverhill, MA) at 1 to 2 kHz and digitized at 4 to 8 kHz. For construction of current amplitude histograms and channel traces, data were filtered at 500 Hz. Channel properties were evaluated with the use of pClamp 6. Open probabilities were determined by analyzing data at 5- and 10-s intervals. The binomial distribution of open probabilities was calculated from the equation

$$P1_{calc} = 2\sqrt{P2}\cdot(1-\sqrt{P2})$$

where $P1_{calc}$ is the calculated open probability of the 4-pA currents and $P2$ is the observed open probability of the 8-pA currents (*10*). The formula is useful when the open probabilities of two channels are approximately equal and pertains to all experimentally observed values for $P2$. Student's t test was used for statistical analysis of the dwell-time distributions and open probabilities.
24. We thank R. Kass, Q. Al-Awqati, S. Siegelbaum, B. Ehrlich, and S. Hamilton for critical reading of the manuscript and for helpful discussions. Supported by NIH grants R01HL56180, R01A139794, and R03TW00949 (A.R.M.), the Muscular Dystrophy Association (A.R.M.), the American Heart Association (A.R.M. and S.O.M.), and the Richard and Lynne Kaiser Family Foundation.

31 December 1997; accepted 24 June 1998

REPORTS

Role of Phosphorylation in Regulation of the Assembly of Endocytic Coat Complexes

Vladimir I. Slepnev, Gian-Carlo Ochoa, Margaret H. Butler, Detlev Grabs, Pietro De Camilli*

Clathrin-mediated endocytosis involves cycles of assembly and disassembly of clathrin coat components and their accessory proteins. Dephosphorylation of rat brain extract was shown to promote the assembly of dynamin 1, synaptojanin 1, and amphiphysin into complexes that also included clathrin and AP-2. Phosphorylation of dynamin 1 and synaptojanin 1 inhibited their binding to amphiphysin, whereas phosphorylation of amphiphysin inhibited its binding to AP-2 and clathrin. Thus, phosphorylation regulates the association and dissociation cycle of the clathrin-based endocytic machinery, and calcium-dependent dephosphorylation of endocytic proteins could prepare nerve terminals for a burst of endocytosis.

Clathrin-mediated endocytosis plays a key role in the recycling of synaptic vesicles in nerve terminals, and several components of the molecular machinery involved in this process have been identified (*1*). These include, in addition to clathrin and the clathrin adaptors, the guanosine triphosphatase dynamin 1, the amphiphysin dimer, and synaptojanin 1. Dynamin 1 oligomerizes into collar structures at the neck of deeply invaginated clathrin-coated pits, and its conformational change is thought to be an essential step leading to vesicle fission (*2*). Synaptojanin 1 is a presynaptic inositol 5-phosphatase enriched on endocytic intermediates (*3*). The amphiphysin dimer (*4*–*6*) binds to both dynamin 1 and synaptojanin 1 through the COOH-terminal SH3 domains of its two subunits (*4*, *7*, *8*). Disruption of SH3-mediated interactions of amphiphysin blocks clathrin-mediated endo-

Howard Hughes Medical Institute and Department of Cell Biology, Yale University School of Medicine, 295 Congress Avenue, New Haven, CT 06510, USA.

*To whom correspondence should be addressed. E-mail: pietro.decamilli@yale.edu

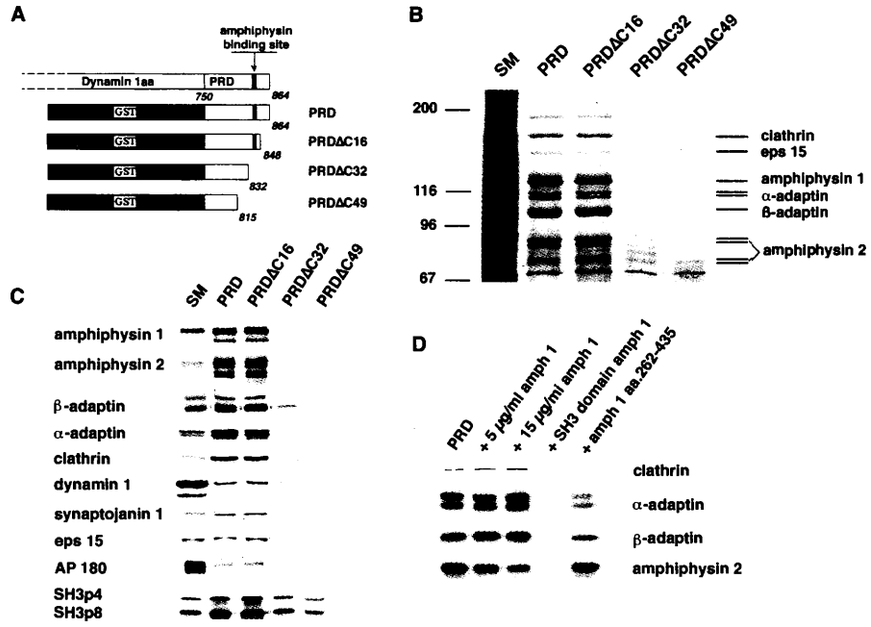

Fig. 1. A macromolecular complex comprising several endocytic proteins can be affinity-purified from a Triton X-100 brain extract by the PRD of dynamin (*13*). (**A**) Schematic drawing of the GST fusion proteins used for affinity chromatography (*8*). (**B**) Coomassie blue staining of the starting rat brain extract and of the material affinity purified by the four constructs shown in (A). (**C**) Immunoblot analysis of the material shown in (B). (**D**) Immunoblot analysis of the material affinity-purified by the PRD in the absence and presence of the indicated amounts of amphiphysin 1, SH3 domain of amphiphysin 1, and central fragment of amphiphysin 1 (amino acids 262 to 435).